Journal of Low Temperature Physics
https://doi.org/10.1007/s10909-022-02775-z

QUBIC Experiment Toward the First Light

G. D'Alessandro[1,2] · E. S. Battistelli[1,2] · P. de Bernardis[1,2] · M. De Petris[1,2] · M. M. Gamboa Lerena[24,33] · L. Grandsire[3], et al. ***[full author details at the end of the article]***

Received: 25 October 2021 / Accepted: 17 June 2022

Abstract
The **Q** & **U** Bolometric Interferometer for Cosmology (QUBIC) is a cosmology experiment that aims to measure the B-mode polarization of the cosmic microwave background (CMB). Measurements of the primordial B-mode pattern of the CMB polarization are in fact among the most exciting goals in cosmology as it would allow testing of the inflationary paradigm. Many experiments are attempting to measure the B-modes, from the ground and the stratosphere, using imaging Stokes polarimeters. The QUBIC collaboration developed an innovative concept to measure CMB polarization using bolometric interferometry. This approach mixes the high sensitivity of bolometric detectors with the accurate control of systematics due to the interferometric layout of the instrument. We present the calibration results for the Technological Demonstrator, before its commissioning in the Argentinian observing site and preparation for first light.

Keywords Instruments: mm-wave · Applications: astrophysics and cosmology

1 Introduction

The Q &U Bolometric Interferometer for Cosmology (QUBIC) is a ground-based experiment which aims to measure the polarization of the cosmic microwave background (CMB). QUBIC uses bolometric interferometry, which combines the calibration control and beam synthesis capabilities of interferometers with bolometric detectors. The main goal of the QUBIC instrument is to detect the polarization pattern hidden in the CMB, known as the primordial B-mode polarization (Hamilton et al. [6]). The detection of this faint signal is strongly affected by instrumental systematic effects and foregrounds. QUBIC, as a bolometric interferometer, can reach the same sensitivity as imagers with the same number of detectors, but it is capable of controlling systematic effects via its *self-calibration* procedure (Tartari et al. [15] and Piat et al. [12]). Thanks to its spectral-imaging capabilities, QUBIC can separate the CMB signal from polarized foregrounds better than an imager experiment (Mousset et al. [10] and Mele et al. [9]). This unique feature of the QUBIC

Published online: 10 August 2022

instrument allows the signal to be extracted in frequency sub-bands within the main channels, with a spectral resolution of $\Delta\nu/\nu \sim 0.05$ (Mousset et al. [10]). In QUBIC, polarization measurement is done using a Stokes polarimeter (a retarder plus a polarizer) as it is in MAXIPOL (Johnson et al. [7]), PILOT (Salatino et al. [14]) and SPIDER (Bryan et al. [2]). The QUBIC polarimeter is composed of a retarder plate, a half-wave plate (HWP), which induces a phase shift between the two orthogonal polarization components, coupled with a linear polarizer that is used as a polarization selector. The current version of the experiment is a Technological Demonstrator (TD) instrument, described in Torchinsky et al. [16], composed of a reduced array of 64 back-to-back feed-horns, one-quarter of the 150 GHz detector array, and a HWP with a reduced diameter compared to the one which will be used in the Full Instrument (FI). This work serves as an overview of the instrument status toward first light, and the subsystems are elaborated on in [3, 4, 6, 8, 10, 13, 16]

2 The QUBIC Instrument

The QUBIC cryostat is composed of three different temperature stages: the vacuum shell at room temperature, the 40 K shield, and the 4 K shield. The internal shields are cooled down through two parallel pulse tube cryocoolers. The vacuum shell is a tall (1.5m) and large (1.4 m diameter) aluminum cylinder with an ultra-high molecular weight (UHMW) polyethylene window [5] followed by two infrared (IR) filters. The 40 K shield is closed by three IR filters, and it is divided from the vacuum shell by 30 superinsulation layers. The 4 K shield is closed by one IR filter and a 360 GHz edge filter. Below this last filter, there is the HWP and the polarizer. The temperature reached by the upper part of the 4 K shield is always between [8,10] K. Inside the 4K shield, there are two fridges: a He4 one, which cools down the optics box and the back-to-back horn array to 1 K, and a He7 one, which cools down the detectors to 340 mK. The horn array and the two mirrors acting as an imager make the system a Fizeau interferometer that is coupled to the sky.

Figure 1 shows the schematic and a sectional cut of the cryostat. Table 1 shows the main parameters of QUBIC-TD and QUBIC-FI.

2.1 Observatory Site

QUBIC will be installed on its final observing site in Argentina at Alto Chorrillos (24 11′S, 66 28′W, 4869 m above sea level) in Salta province. The site has an excellent sky. The measured sky opacity at 210 GHz is < 0.1 (50th percentile). The average atmospheric temperature is 270 K with an emissivity of 0.081 and 0.138 at 150 GHz and 220 GHz, respectively.

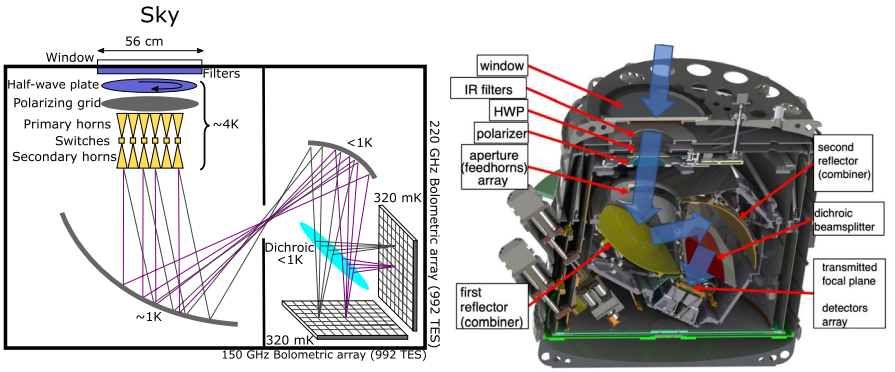

Fig. 1 Schematic of the QUBIC instrument (left) and sectional cut of the cryostat (right) showing the same sub-systems in their real configuration (Color figure online).

Table 1 QUBIC main parameters

Parameter	TD (measured)	FI (forecasted)
Frequency channels	150 GHz	150 and 220 GHz
Frequency range 150 GHz	[131–169] GHz	[131–169] GHz
Frequency range 220 GHz	–	[192.5–247.5] GHz
Window aperture [m]	0.56	0.56
Number of horns	64	400
Number of detectors	248	992×2
Detector noise [W/$\sqrt{\text{Hz}}$]	2.05×10^{-16} [13]	4.7×10^{-17}
Focal plane temp. [mK]	340 [8]	300
Synthesized beam FWHM [deg]	0.68 [16]	0.39 (150 GHz), 0.27 (220 GHz)

2.2 TD Forecast and Strategy Scan

The main goal of QUBIC-TD was to validate the technology before updating the instrument to its final configuration (FI). QUBIC-TD aimed to demonstrate bolometric interferometry and spectral imaging by using the spectral dependence of the synthesized beam and the systematic effect removal thanks to self-calibration. A good test-bed for this is the polarized component of the dust. We simulated 1 year of observation of the galactic plane center with QUBIC-TD, showing the capability of the instrument to reconstruct the spectral energy distribution of the dust [6]. QUBIC-FI will observe a sky patch at mid galactic latitudes in the southern hemisphere, 35° in azimuth and 40° in elevation, including the BICEP2 region (RA = 0°, dec = −57°) and the Planck clean field (RA = 8.7°, dec = −41.7°). QUBIC will scan the sky quickly by moving in azimuth at a speed of 0.4/s and will change the HWP position after each scan. QUBIC will use the

slewing time to step the HWP angle by 15°. It will also spend part of its observing time performing the self-calibration as described in Bigot-Sazy et al. [1]. This procedure, combined with the possibility of rotating the instrument around its optical axis (boresight axis), helps monitor systematic effects.

3 Calibration Results

QUBIC-TD has been tested during a calibration campaign, with the focal plane cooled down to 340 mK and with the HWP rotator at a temperature of 8 K. The measurements were performed by setting the calibration source frequency to 150 GHz. The calibration source consists of a 12 GHz synthesizer followed by two multipliers that increase the operating frequency into the 130–170 GHz band (VDI electronics). The source waveguide is coupled to a conical corrugated horn using a rectangular-to-circular transition and is linearly polarized with cross-polarization and return loss. During the first calibration phase, a cold neutral density filter (9% transmission) was placed at 4 K. During the calibration phase, all the subsystems were successfully tested, as summarized below and described in more detail in Torchinsky et al. [16]. Additional tests will be performed at the laboratory in Salta before bringing the experiment to its observation site. These tests will include full-beam calibration by illuminating the focal plane with a polarized emitting black body. The full-beam calibrator consists of a baffle placed directly in front of the QUBIC-TD window with a rotating polarizer which allows the polarization to be measured by modulating the input polarization. Measurement at different frequencies will perform again to better test the spectro-imaging feature of QUBIC-TD.

3.1 Detector Performances

QUBIC-TD has only a quarter of the QUBIC-FI focal plane: the detection chain is currently made of 256 NbSi Transition Edge Sensors cooled to 340 mK. The readout system is a 128:1 time-domain multiplexing scheme based on 128 SQUIDs cooled to 1 K. The QUBIC detection chain based on TES and SQUID has reached an important milestone. We demonstrated an overall yield of approximately 80% of working detectors (TESs and SQUIDs included), compatible with a phonon noise of about 5×10^{-17} W$/\sqrt{\text{Hz}}$ at a 410 mK critical temperature. The time constant is about 40 ms. The QUBIC sensitivity is, however, currently limited to 2×10^{-16} W$/\sqrt{\text{Hz}}$ by microphonic noise and aliasing in the readout electronics [13].

3.2 Optics

The sky is coupled to the cold optics by a back-to-back horn array [3], and the two cold mirrors make up a Fizeau Interferometer [11]. The synthetic beam has been successfully measured for a pixel near the center of the focal plane at 150 GHz. Figure 2 shows good agreement between the measured beam and the theoretical prediction, including aberrations. More detail on the optics is given in [11].

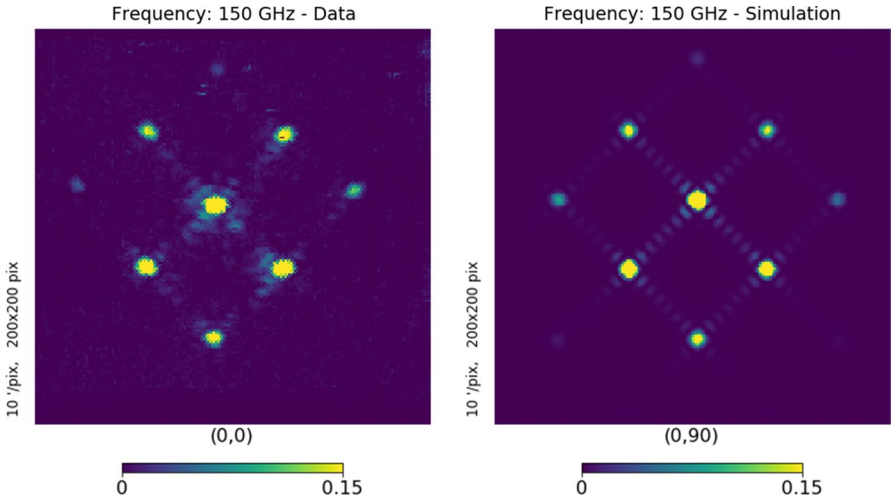

Fig. 2 QUBIC synthesized beam on the sky (left: laboratory measurement with the TD, right: simulations without optical aberrations) at 150 GHz. Note that the color scales are arbitrary units. Details on this measurement can be found in Torchinsky et al. [16] from this series of articles. The synthesized beam shrinks with increasing frequency as can be seen with the animated version of this image that can be found online at https://box.in2p3.fr/index.php/s/bzPYfmtjQW4wCGj (Color figure online).

3.3 Polarization Modulation

An important feature of an experiment which aims to measure the polarized B-mode of the CMB is the capability to modulate the polarization. A cross-polarization of less than 1% has been measured for more than 80% of detectors at 150 GHz [4]. The mean value over the focal plane is 0.12%. The polarization efficiency for the detectors with the best signal-to-noise ratio ($S/N > 5$) is always $> 99\%$ (68% C.L.) when the non-linear model is included.

The cryogenic rotator has a clear aperture of 370 mm, sufficient for the HWP of QUBIC-FI, and can rotate at 7.5°/s, with no data-loss and no cryogenic issues detected. We estimate < 5.0 mW (95% C.L.) is dissipated on the cryogenic stage during operation, satisfying the low-temperature requirement. It is placed at the top of the 4K stage, after the IR blocker filters, as described in Masi et al. [8]. The rotation is produced by an external stepper motor, placed on the top of the cryostat vacuum shell. It is transmitted to the HWP through two magnetic joints and a fiberglass tube shaft combined with a system of pulleys and a stainless steel belt.

The time-ordered data (TOD) acquired at the seven nominal rotator positions were first processed using Fourier transforms to calculate power spectra. An exponential fit, applied to the spectra but excluding the main peak from the 1 Hz modulated input source, was used to estimate the noise level of each acquisition by integrating over the main band [0.7, 1.3] Hz.

The modulation has been processed with two models:

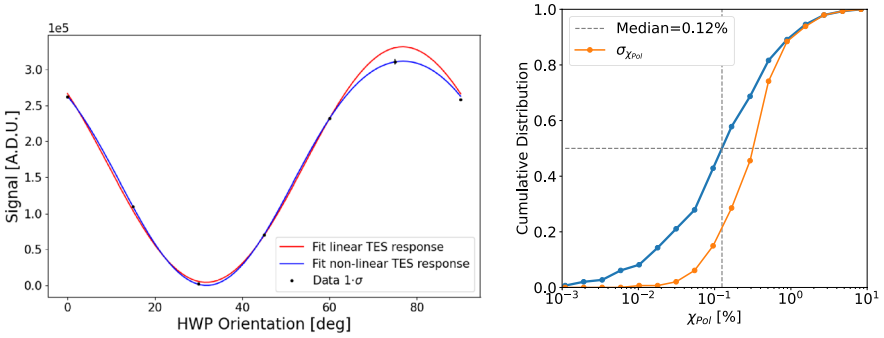

Fig. 3 *(left)* Polarization modulation curves acquired at the nominal HWP positions $[0°, 15°, 30°, 45°, 60°, 75°, 90°]$, for a typical TES detectors at different locations in the focal plane and given in Arbitrary Digital Units. Data points are estimated via integration of the TOD Fourier transform over the band [0.7, 1.3] Hz at each nominal HWP position. Two models are used to fit the data: a model as in Eq. (1) (red line) and a model where the response of the detector is included as a function which deviates from linearity for high input power, as in Eq. (2) (blue line). *(right)* Cumulative distribution for the cross-pol (blue) and the cumulative distribution of the cross-pol 1-σ error (orange) (Color figure online)

$$I = \text{eff} \cdot \frac{1}{2}[T + Q\cos(4\theta + \phi)] \tag{1}$$

where pure linearly polarized light is assumed as input, but with a still unknown polarization angle, determined by the experimental setup alignment. To include the detector response, we consider the model:

$$I' = k \cdot \tanh(I/k) \tag{2}$$

which grows linearly with the signal in the limit $I \ll k$ and tends to k for $I \gg k$, where I is the modulated intensity of Eq. (1), and k is the saturation parameter(Fig. 3).

4 Conclusions

QUBIC-TD has been successfully tested during a long calibration phase: from the optical point of view, the synthesized beam has been measured at different frequencies and is in agreement with theory [11, 16]; the detector NEP is 2×10^{-16} W/$\sqrt{\text{Hz}}$ limited by microphonic noise and aliasing in the readout electronics [13]; and the average cross-polarization is 0.12% [4] A dedicated laboratory has been built near the observatory site at Salta in Argentina. After a short phase of new tests in this laboratory, the instrument will be brought to its observatory site at Alto Chorrillos for the first light. QUBIC-TD will take 6 months of measurement and after it will be updated to its final version with a bigger filter, bigger HWP and two complete focal planes. After the instrument update, there will be a scientific commissioning phase

without removing the instrument from the observatory site and using a calibration source placed on a 50-m high tower to calibrate the experiment. The same calibration source will be used for the self-calibration procedure. QUBIC-FI first light is expected in the first half of 2023.

References

1. M.A. Bigot-Sazy, R. Charlassier, J.C. Hamilton, J. Kaplan, G. Zahariade, Self-calibration: an efficient method to control systematic effects in bolometric interferometry. Astron. Astrophys. **550**, A59 (2013). https://doi.org/10.1051/0004-6361/201220429
2. S.A. Bryan, T.E. Montroy, J.E. Ruhl, Modeling dielectric half-wave plates for cosmic microwave background polarimetry using a Mueller matrix formalism. Appl. Opt. **49**(32), 6313–6323 (2010). https://doi.org/10.1364/AO.49.006313
3. F. Cavaliere, A. Mennella, M. Zannoni, et al. QUBIC VII: the feedhorn-switch system of the technological demonstrator (2020). arXiv e-prints arXiv:2008.12721
4. G. D'Alessandro, L. Mele, F. Columbro, et al. QUBIC VI: cryogenic half wave platerotator, design and performances (2020). arXiv e-prints arXiv:2008.10667
5. G. D'Alessandro, A. Paiella, A. Coppolecchia, M.G. Castellano, I. Colantoni, P. de Bernardis, L. Lamagna, S. Masi, Ultra high molecular weight polyethylene: optical features at millimeter wavelengths. Infrared Phys. Technol. **90**, 59–65 (2018). https://doi.org/10.1016/j.infrared.2018.02.008
6. J.C. Hamilton, L. Mousset, et al. QUBIC I: overview and ScienceProgram (2020). arXiv e-prints arXiv:2011.02213
7. ...B.R. Johnson, J. Collins, M.E. Abroe, P.A.R. Ade, J. Bock, J. Borrill, A. Boscaleri, P. de Bernardis, S. Hanany, A.H. Jaffe, T. Jones, A.T. Lee, L. Levinson, T. Matsumura, B. Rabii, T. Renbarger, P.L. Richards, G.F. Smoot, R. Stompor, H.T. Tran, C.D. Winant, J.H.P. Wu, J. Zuntz, MAXIPOL: cosmic microwave background polarimetry using a rotating half-wave plate. Astrophys. J. **665**(1), 42–54 (2007). https://doi.org/10.1086/518105
8. S. Masi, et al.: QUBIC V: cryogenic system design and performance (2020). arXiv e-prints arXiv:2008.10659
9. L. Mele, P. Ade, J.G. Alberro, A. Almela, G. Amico, L.H. Arnaldi, D. Auguste, J. Aumont, S. Azzoni, S. Banfi, E.S. Battistelli, A. Baù, B. Bèlier, D. Bennett, L. Bergé, J.P. Bernard, M. Bersanelli, M.A. Bigot-Sazy, N. Bleurvacq, J. Bonaparte, J. Bonis, A. Bottani, E. Bunn, D. Burke, D. Buzi, F. Cavaliere, P. Chanial, C. Chapron, R. Charlassier, F. Columbro, A. Coppolecchia, G. D'Alessandro, P. de Bernardis, G. De Gasperis, M. De Leo, M. De Petris, S. Dheilly, L. Dumoulin, A. Etchegoyen, A. Fasciszewski, L.P. Ferreyro, D. Fracchia, C. Franceschet, M.M. Gamboa Lerena, K. Ganga, B. García, M.E. García Redondo, M. Gaspard, D. Gayer, M. Gervasi, M. Giard, V. Gilles, Y. Giraud-Heraud, M. Gómez Berisso, M. González, M. Gradziel, L. Grandsire, J.C. Hamilton, D. Harari, S. Henrot-Versillé, D.T. Hoang, F. Incardona, E. Jules, J. Kaplan, C. Kristukat, L. Lamagna, S. Loucatos, T. Louis, B. Maffei, S. Marnieros, W. Marty, S. Masi, A. Mattei, A. May, M. McCulloch, S. Melhuish, A. Mennella, L. Montier, L. Mousset, L.M. Mundo, J.A. Murphy, J.D. Murphy, F. Nati, E. Olivieri,C. Oriol, C. O'Sullivan, A. Paiella, F. Pajot, A. Passerini,H. Pastoriza, A. Pelosi, C. Perbost, M. Perciballi, F. Pezzotta, F. Piacentini, M. Piat, L. Piccirillo, G. Pisano, M. Platino, G. Polenta, D. Prêle, R. Puddu, D. Rambaud, P. Ringegni, G.E. Romero, M. Salatino, J.M. Salum, A. Schillaci, C. Scóccola, S. Scully, S. Spinelli, G. Stankowiak, M. Stolpovskiy, A. Tartari,J.P. Thermeau, P. Timbie, M. Tomasi, S. Torchinsky, M. Tristram, G. Tucker, C. Tucker, D. Viganò, N. Vittorio, F. Voisin, F. Wicek, M. Zannoni, A. Zullo, The QUBIC instrument for CMB polarization measurements. J. Phys. Conf. Ser. **1548**, 012016 (2020). https://doi.org/10.1088/1742-6596/1548/1/012016
10. L. Mousset, M.M. Gamboa Lerena, et al. QUBIC II: spectro-polarimetry with bolometric interferometry. arXiv e-prints arXiv:2010.15119 (2020)
11. C. O'Sullivan, M. De Petris, et al. QUBIC VIII: optical design and performance (2020). arXiv e-prints arXiv:2008.10119
12. ...M. Piat, E. Battistelli, A. Baù, D. Bennett, L. Bergé, J.P. Bernard, P. de Bernardis, M.A. Bigot-Sazy, G. Bordier, A. Bounab, E. Bréelle, E.F. Bunn, M. Calvo, R. Charlassier, S. Collin, A.

Cruciani, G. Curran, L. Dumoulin, A. Gault, M. Gervasi, A. Ghribi, M. Giard, C. Giordano, Y. Giraud-Héraud, M. Gradziel, L. Guglielmi, J.C. Hamilton, V. Haynes, J. Kaplan, A. Korotkov, J. Landé, B. Maffei, M. Maiello, S. Malu, S. Marnieros, J. Martino, S. Masi, L. Montier, A. Murphy, F. Nati, C. O'Sullivan, F. Pajot, C. Parisel, A. Passerini, S. Peterzen, F. Piacentini, L. Piccirillo, G. Pisano, G. Polenta, D. Prêle, D. Romano, C. Rosset, M. Salatino, A. Schillaci, G. Sironi, R. Sordini, S. Spinelli, A. Tartari, P. Timbie, G. Tucker, L. Vibert, F. Voisin, R.A. Watson, M. Zannoni, QUBIC: the Q &U bolometric interferometer for cosmology. J. Low Temp. Phys. **167**, 872–878 (2012). https://doi.org/10.1007/s10909-012-0522-x

13. M. Piat, G. Stankowiak, et al. QUBIC IV: performance of TES bolometers and readout electronics (2021). arXiv e-prints arXiv:2101.06787
14. M. Salatino, P. de Bernardis, S. Masi, A cryogenic waveplate rotator for polarimetry at mm and submm wavelengths. A &A **528**, A138 (2011). https://doi.org/10.1051/0004-6361/201015288
15. ...A. Tartari, J. Aumont, S. Banfi, P. Battaglia, E.S. Battistelli, A. Baù, B. Bélier, D. Bennett, L. Bergé, J.P. Bernard, M. Bersanelli, M.A. Bigot-Sazy, N. Bleurvacq, G. Bordier, J. Brossard, E.F. Bunn, D. Buzi, D. Cammilleri, F. Cavaliere, P. Chanial, C. Chapron, A. Coppolecchia, G. D'Alessandro, P. De Bernardis, T. Decourcelle, F. Del Torto, M. De Petris, L. Dumoulin, C. Franceschet, A. Gault, D. Gayer, M. Gervasi, A. Ghribi, M. Giard, Y. Giraud-Héraud, M. Gradziel, L. Grandsire, J.C. Hamilton, V. Haynes, N. Holtzer, J. Kaplan, A. Korotkov, J. Lande, A. Lowitz, B. Maffei, S. Marnieros, J. Martino, S. Masi, M. McCulloch, S. Melhuish, A. Mennella, L. Montier, A. Murphy, D. Néel, M.W. Ng, C. O'Sullivan, F. Pajot, A. Passerini, C. Perbost, F. Piacentini, M. Piat, L. Piccirillo, G. Pisano, D. Prêle, D. Rambaud, O. Rigaut, M. Salatino, A. Schillaci, S. Scully, M.M. Stolpovskiy, P. Timbie, G. Tucker, D. Viganò, F. Voisin, B. Watson, M. Zannoni, QUBIC: a Fizeau interferometer targeting primordial B-modes. J. Low Temp. Phys. **184**, 739–745 (2016). https://doi.org/10.1007/s10909-015-1398-3
16. S.A. Torchinsky, et al.: QUBIC III: laboratory characterization (2020). arXiv e-prints arXiv:2008.10056

Authors and Affiliations

G. D'Alessandro[1,2] · E. S. Battistelli[1,2] · P. de Bernardis[1,2] · M. De Petris[1,2] · M. M. Gamboa Lerena[24,33] · L. Grandsire[3] · J.-Ch. Hamilton[3] · S. Marnieros[4] · S. Masi[1,2] · A. Mennella[5,6] · L. Mousset[3] · C. O'Sullivan[7] · M. Piat[3] · A. Tartari[9] · S. A. Torchinsky[3,10] · F. Voisin[3] · M. Zannoni[11,12] · P. Ade[8] · J. G. Alberro[13] · A. Almela[14] · G. Amico[1] · L. H. Arnaldi[15] · D. Auguste[4] · J. Aumont[16] · S. Azzoni[17] · S. Banfi[11,12] · A. Baù[11,12] · B. Bélier[18] · D. Bennett[7] · L. Bergé[4] · J.-Ph. Bernard[16] · M. Bersanelli[5,6] · M.-A. Bigot-Sazy[3] · J. Bonaparte[19] · J. Bonis[4] · E. Bunn[20] · D. Burke[7] · D. Buzi[1] · F. Cavaliere[5,6] · P. Chanial[3] · C. Chapron[3] · R. Charlassier[3] · A. C. Cobos Cerutti[14] · F. Columbro[1,2] · A. Coppolecchia[1,2] · G. De Gasperis[21,22] · M. De Leo[1,23] · S. Dheilly[3] · C. Duca[14] · L. Dumoulin[4] · A. Etchegoyen[14] · A. Fasciszewski[19] · L. P. Ferreyro[14] · D. Fracchia[14] · C. Franceschet[5,6] · K. M. Ganga[3] · B. García[14] · M. E. García Redondo[14] · M. Gaspard[4] · D. Gayer[7] · M. Gervasi[11,12] · M. Giard[16] · V. Gilles[1,25] · Y. Giraud-Heraud[3] · M. Gómez Berisso[15] · M. González[15] · M. Gradziel[7] · M. R. Hampel[14] · D. Harari[15] · S. Henrot-Versillé[4] · F. Incardona[5,6] · E. Jules[4] · J. Kaplan[3] · C. Kristukat[26] ·

L. Lamagna[1,2] · S. Loucatos[3,27] · T. Louis[4] · B. Maffei[28] · W. Marty[16] · A. Mattei[2] · A. May[25] · M. McCulloch[25] · L. Mele[1,2] · D. Melo[14] · L. Montier[16] · L. M. Mundo[13] · J. A. Murphy[7] · J. D. Murphy[7] · F. Nati[11,12] · E. Olivieri[4] · C. Oriol[4] · A. Paiella[1,2] · F. Pajot[16] · A. Passerini[11,12] · H. Pastoriza[15] · A. Pelosi[2] · C. Perbost[3] · M. Perciballi[2] · F. Pezzotta[5,6] · F. Piacentini[1,2] · L. Piccirillo[25] · G. Pisano[1,8] · M. Platino[14] · G. Polenta[1,29] · D. Prêle[3] · G. Presta[1,2] · R. Puddu[1,30] · D. Rambaud[16] · E. Rasztocky[31] · P. Ringegni[13] · G. E. Romero[31] · J. M. Salum[14] · A. Schillaci[1,32] · C. G. Scóccola[24,33] · S. Scully[7,34] · S. Spinelli[11] · G. Stankowiak[3] · M. Stolpovskiy[3] · A. D. Supanitsky[14] · J.-P. Thermeau[3] · P. Timbie[35] · M. Tomasi[5,6] · G. Tucker[36] · C. Tucker[8] · D. Viganò[5,6] · N. Vittorio[21] · F. Wicek[4] · M. Wright[25] · A. Zullo[2]

✉ G. D'Alessandro
giuseppe.dalessandro@uniroma1.it

[1] Università di Roma - La Sapienza, Rome, Italy

[2] INFN sezione di Roma, 00185 Rome, Italy

[3] CNRS, Astroparticule et Cosmologie, Université de Paris, 75006 Paris, France

[4] Laboratoire de Physique des 2 Infinis Irène Joliot-Curie (CNRS-IN2P3, Université Paris-Saclay), Orsay, France

[5] Università degli studi di Milano, Milan, Italy

[6] INFN sezione di Milano, 20133 Milan, Italy

[7] National University of Ireland, Maynooth, Ireland

[8] Cardiff University, Cardiff, UK

[9] INFN sezione di Pisa, 56127 Pisa, Italy

[10] Observatoire de Paris, Université Paris Science et Lettres, 75014 Paris, France

[11] Università di Milano - Bicocca, Milan, Italy

[12] INFN sezione di Milano - Bicocca, 20216 Milan, Italy

[13] GEMA (Universidad Nacional de La Plata), La Plata, Argentina

[14] Instituto de Tecnologías en Detección y Astropartículas (CNEA, CONICET, UNSAM), Buenos Aires, Argentina

[15] Centro Atómico Bariloche and Instituto Balseiro (CNEA), San Carlos de Bariloche, Argentina

[16] Institut de Recherche en Astrophysique et Planétologie (CNRS-INSU), Toulouse, France

[17] Department of Physics, University of Oxford, Oxford, UK

[18] Centre de Nanosciences et de Nanotechnologies, Orsay, France

[19] Centro Atómico Constituyentes (CNEA), Villa Maipú, Argentina

[20] University of Richmond, Richmond, USA

[21] Università di Roma "Tor Vergata", Rome, Italy

[22] INFN sezione di Roma2, 00133 Rome, Italy

[23] University of Surrey, Guildford, UK

[24] Facultad de Ciencias Astronómicas y Geofísicas (Universidad Nacional de La Plata), La Plata, Argentina

[25] University of Manchester, Manchester, UK

[26] Escuela de Ciencia y Tecnología (UNSAM) and Centro Atómico Constituyentes (CNEA), Villa Lynch, Argentina

[27] IRFU, CEA, Université Paris-Saclay, 91191 Gif-sur-Yvette, France

[28] Institut d'Astrophysique Spatiale (CNRS-INSU), Orsay, France

[29] Italian Space Agency, Rome, Italy

[30] Pontificia Universidad Catolica de Chile, Santiago, Chile

[31] Instituto Argentino de Radioastronomía (CONICET, CIC, UNLP), Pereyra, Argentina

[32] California Institute of Technology, Pasadena, USA

[33] CONICET, Buenos Aires, Argentina

[34] Institute of Technology, Carlow, Ireland

[35] University of Wisconsin, Madison, USA

[36] Brown University, Providence, USA